Available online at www.sciencedirect.com
SCIENCE DIRECT®
Journal of the European Ceramic Society 25 (2005) 425–432
www.elsevier.com/locate/jeurceramsoc

# Effects of uniaxial prestress on the ferroelectric hysteretic response of soft PZT

Dayu Zhou*, Marc Kamlah, Dietrich Munz

*Forschungszentrum Karlsruhe, Institut fuer Materialforschung II, D-76021 Karlsruhe, Germany*

Received 29 November 2003; accepted 25 January 2004
Available online 21 July 2004

**Abstract**

This paper deals with the influence of preload stress on the ferroelectric hysteretic behavior of piezoelectric ceramics. The polarization and strain versus electric field hysteresis loops were measured for soft lead zirconate titanate (PZT) piezoceramic material under various uniaxial compressive stress preloads of up to −400 MPa. The investigation revealed that the superimposed compression load reduced the remnant polarization, decreased the coercive field, and also had a significant impact on the dielectric and piezoelectric properties. With increasing mechanical load, dielectric hysteresis and butterfly hysteresis became less and less pronounced, as the compressive stress prevented full alignment of the domains and induced mechanical depolarization. The slopes of the polarization and strain curves at zero electric field were measured to evaluate the dependence of permittivity and piezoelectric coefficients on the prestress. The experimental results were interpreted in terms of the non-180° domain switching process under combined electromechanical loading.
© 2004 Elsevier Ltd. All rights reserved.

*Keywords:* PZT; Piezoceramics; Domain switching; Polarization; Strain; Preload stress; Dielectric and piezoelectric properties

## 1. Introduction

Lead zirconate titanate (PZT) ceramics are widely used in sensor and actuator applications as a representative piezoelectric material.[1–3] To enhance electro-mechanical coupling, most of the technically important PZT ceramics have compositions in the vicinity of the morphotropic phase boundary (MPB), with two ferroelectric phases, i.e., the tetragonal and the rhombohedral phases, coexisting inside the materials.[4,5] PZT ceramics are usually modified with dopants to meet the stringent requirements for specific applications. In general, high-valent additives (donors) induce “soft” piezoelectric behavior, while lower valent additives (acceptors) induce “hard” behavior.[3–5] The higher piezoelectric coefficients of soft compositions are appropriate for positioning actuator applications, while hard PZT ceramics are particularly suitable for ultrasonic motor applications.[2]

Polycrystalline ferroelectric ceramics consist of crystals subdivided into domains separated by domain walls. A domain is a group of unit cells within a single crystal all of which share the same spontaneous polarization direction. Based on the angle between polarization directions in neighboring domains, domain walls can be grouped into two categories: 180° walls separating domains with opposite polarization vectors, and non-180° walls separating the remaining domains (90° for tetragonal symmetry and 71°/109° for rhombohedral symmetry).[4,5] Application of an electric field or a mechanical load above a critical magnitude may reorientate the polarization direction of domains. This effect is commonly called domain switching or domain wall motion. Domain switching induced by electric field loading is referred to as ferroelectric switching; both 180° and non-180° reorientation can occur in this case. Piezoceramics also exhibit ferroelasticity, where non-180° domain switching can be induced by mechanical stress loading of sufficient magnitude.[6] The consequence of domain switching is the occurrence of non-linear hysteresis behavior.

For piezoceramic materials working under high-frequency, small-signal loading conditions, a set of linear constitutive laws has been developed to describe the electromechanical coupling behavior, and the material parameters are normally determined by weak-field measurements performed using a resonance-antiresonance method.[7] However, nowadays, piezoelectric actuators normally have complicated

* Corresponding author. Tel.: +49-7247-82-5855; fax: +49-7247-82-2347.
*E-mail address:* dayu.zhou@imf.fzk.de (D. Zhou).

0955-2219/$ – see front matter © 2004 Elsevier Ltd. All rights reserved.
doi:10.1016/j.jeurceramsoc.2004.01.016

geometries and are required to work under severe loading conditions. For instance, some active actuator applications (e.g., vibration suppression devices, sonar projectors, etc.) require the active material to accommodate significant compression preloads and produce high strain outputs. To accomplish this, a strong electric field must be applied.[8–10] For components with field intensifiers, e.g., cracks or embedded electrodes, local stress or electric field concentrations will occur inside the structure.[11–13]

When large-signal loads (electric field and/or stress) are applied, the real responses of piezoceramics are dominated by a significant non-linearity and hysteresis due to the inherent ferroelectricity and ferroelasticity. Consequently, the conventional linear assumptions for small-signal loading conditions are inadequate in representing accurately the practical behavior of materials. For device design, working condition optimization and, especially, for components reliability assessment, recent experimental and modeling efforts focused on evaluating and understanding the large-signal non-linear behavior of ferroelectric piezoceramics in the context of domain switching.

In general, the constitutive models describing the hysteresis properties of piezoceramics fall into one of two classes: Phenomenological models and micro-mechanical models. The review article by Kamlah[14] discussed details of the material behavior and recent constitutive modeling efforts.

On the experimental side, Cao and Evans[11] studied the response of soft and hard PZT piezoceramics to uniaxial compressive stress loading. When a sufficiently high compressive load was applied, the stress–strain behavior was characterized by significant non-linearity with a distinct irreversible remnant strain present upon unloading. In addition, non-linear mechanical depolarization was induced also for the pre-polarized specimen. These non-linear responses were attributed to ferroelastic non-180° domain switching processes. Fett and coworkers[15,16] compared the non-linear response of soft PZT ceramics under tensile and compressive loading. Due to the different ferroelastic domain switching processes in tension and compression, a non-symmetric deformation behavior was observed; the tensile strength was found to be much lower than the compressive strength. Partial unloading tests were further performed to measure the change of Young's modulus under uniaxial compressive stress loading. Young's modulus was found to increase from 40–70 GPa (depending on the poling states) up to about 130–150 GPa with increasing stresses. Schäufele and Härdtl[12] investigated the effects of a biasing electric field on the compressive non-linear behavior of PZT ceramics with variable Zr:Ti ratios and additive dopants. An electric field applied parallel to the poling direction was found to linearly increase the coercive stress of ferroelastic switching.

Applying a strong alternating electric field to a mechanically unclamped piezoceramic specimen causes the polarization to reverse. As a result, the plots of polarization and strain versus the field applied are recorded by the so-called dielectric and "butterfly" strain hysteresis loops. This pure ferroelectric hysteresis behavior were investigated extensively by materials scientists.[3–5,17] Additionally, it was found that the hysteresis response of piezoceramics depended significantly on the amplitude and frequency of the field applied.[18,19] For active actuator applications and reliability assessment of components referred to above, several authors studied ferroelectric behavior as a function of mechanical preloads. Lynch[20] measured the polarization and strain versus electric field hysteresis loops for (Pb,La)(Zr,Ti)$O_3$ (PLZT) ceramics at various compression preload levels of up to −60 MPa. The effects of prestress on remnant polarization, the coercive field, and piezoelectric coefficients were studied qualitatively. It is worth noting that PLZT is a kind of very soft relaxor ferroelectric material. It is convenient to deal for experiments (quite easier to be poled by low electric field application and depoled by small mechanical load), but is not of interest in practical piezoelectric actuator applications. Recently, Chaplya and Carman[21] presented similar experimental results for the non-linear electromechanical behavior of PZT-5H soft piezoceramics. In their work, polarization and strain responses to bilpoar and unipolar electric field loading were evaluated at various prestresses of up to −175 MPa, and the measurement results were interpreted qualitatively in terms of two successive non-180° domain switching processes. Although these investigations provided valuable information on the non-linear behavior of piezoceramics, they were performed within a limited compressive preload range, and only part of the properties were characterized.

To compensate for the noticeable lack of experimental data about the non-linear properties of piezoceramics, the polarization as well as the longitudinal and transverse strains versus full cycles of electric field hysteresis loops were systematically measured in this study for a commercial soft PZT ceramic over a wide range of uniaxial compressive preloads. Based on the measurement results, the influence of prestress on dielectric permittivity, the piezoelectric constants, $d_{33}$ and $d_{31}$, was determined by plotting the slopes of the hysteresis curves at zero field. The experimental results were explained physically in terms of two successive non-180° domain switching processes under combined electromechanical loading. This type of investigation can serve to calibrate the existing models and develop a more suitable constitutive law for the complete response of piezoceramics over a wide range of environmental conditions and signals applied.

## 2. Experimental procedures

### 2.1. Material, specimen preparation, and experimental setup

Measurements were performed on a commercially available PIC 151 piezoceramic (PI Ceramic, Germany). This material is a kind of $Pb(Ni_{1/3}Sb_{2/3})O_3$–$PbTiO_3$–$PbZrO_3$ ternary phase system incorporating approximately 2–3% of $Pb(Ni_{1/3}Sb_{2/3})O_3$ in the vicinity of the morphotropic phase boundary (MPB) of PZT in the tetragonal range.[22] $Sb^{5+}$ in the composition acts as a donor to make the material "soft." Therefore, the material may be considered a kind of soft PZT. For further information about this material, see www.piceramic.de.

The samples were cut and ground by the manufacturer into rectangular blocks of 5 mm × 5 mm × 15 mm, with silver electrodes burnt into the top and bottom 5 mm × 5 mm surfaces. The large aspect ratio of 3:1 can ensure that a significant middle portion of the sample experiences uniform uniaxial stress and strain states.

The external load-induced deformations were monitored by a strain gauge technique using an M-bond 600 adhesive (Vishay Measurements Group). A pair of strain gauges mounted on opposite sides were used to measure the longitudinal strain; another two gauges were employed for transverse strain monitoring. Initial investigations indicated that the deformation signal detected by strain gauges could differ significantly from the true strain when the electric field applied became very strong. This challenge was eventually solved by attaching a thin layer of Kapton polyimide film between the sample and the gauges. Theoretical analysis indicated that this polyimide substrate could provide sufficient insulation of the conductive gauge pattern to avoid electric field distortion in the PZT ceramics and, consequently, could ensure correct strain measurement.[23]

As is shown in Fig. 1, a special experimental setup was developed for simultaneous application of the stress and the electric field. A fluorinert electric liquid (FC-40, 3 M) bath was designed to prevent high-voltage arcing during electric loading. A uniaxial compressive stress was supplied by the Instron servohydraulic load frame (Model 1361). The top fixture incorporated a spherical joint assembly to accommodate slight misalignment. The prepared specimen was carefully placed in the center between two flat alumina blocks insulating the load frame from high voltage. High voltage was provided by a bipolar high-voltage power supply with a maximum output of ±30 kV (HCB 15-30 000, F. u. G., Germany) and applied to the specimen via the copper shims attached to the alumina blocks.

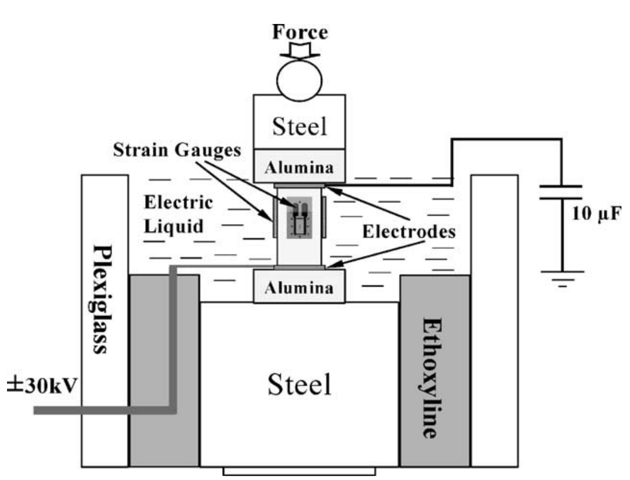


Fig. 1. Experimental setup used for the combined electromechanical tests.

Electric polarization was measured by a modified Sawyer–Tower circuit. A high input resistance electrometer (6517A, Keithley Instruments) was employed to monitor voltage fluctuations across a 10 μF reference capacitor connected in series with the specimen.

KWS 3073 5 kHz carrier frequency amplifiers (Hottinger Baldwin Messtechnik, Germany) were used to monitor strain. Prior to each experiment, the specimen was first subjected to a very low compression load, after which the strain readings from each pair of opposed strain gauges were compared to detect the degree of bending introduced in the sample. When the difference in strains indicated by one pair of gauges was too large, the specimen position was readjusted carefully and the entire procedure was repeated. Only when it was certain that a uniaxial compressive stress was applied along the central specimen axis, could the measurement begin. To further minimize bending effects, the data recorded by each pair of strain gauges were averaged to plot the curves after the experiment.

A computer equipped with a data acquisition board and running DASYLAB software (National Instruments) was used to control simultaneously the Instron machine and the high-voltage power supply. All equipment output signals were first passed through insulated dc input/output signal-conditioning modules (Phoenix Contact, Germany) and then digitally recorded by DASYLAB. The signal-conditioning modules served to further insulate the computer against high-voltage discharges.

Further details of the method of specimen preparation and the electromechanical test setup can be found in Ref. 23.

### *2.2. Measurement procedure*

The experiment was performed on initially unpolarized specimens; full cycles of a ramp-shaped electric field were applied to the sample under different co-axial compressive stress preloads. Starting the loading in positive direction, the $E$ field amplitude range was limited between +2 and −2 kV/mm, with a loading rate of 0.08 kV/mm per second. The magnitude of the discretely preloaded constant stress varied from 0 to −400 MPa; the loading rate was 5 MPa/s between two steps. Polarization as well as longitudinal and transverse strains versus electric field hysteresis loops were monitored simultaneously. To take into account time-dependent effects of depolarization and strain responses under constant mechanical load,[23,24] increasing the preload stress to a new magnitude included a holding time of 150 s before electric field cycling was started. A total of four cycles of the electric field were applied to the specimen at each constant prestress level, and only the curves induced during the last cycle were plotted for illustration. The measurements were repeated three to four times to ensure reliability of the experimental findings.

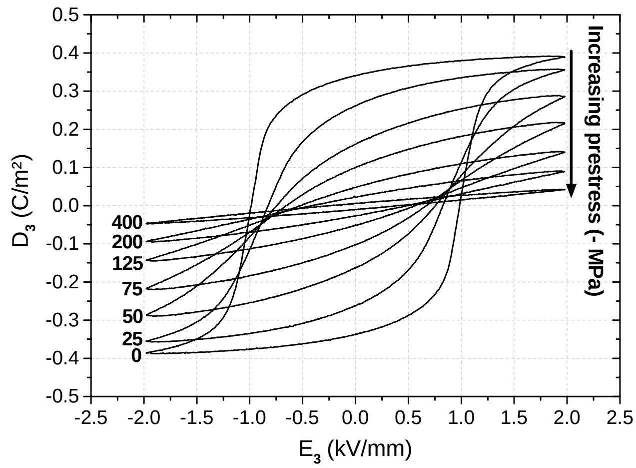


Fig. 2. Polarization vs. electric field (*P–E*) hysteresis loops as a function of compressive stress preload.

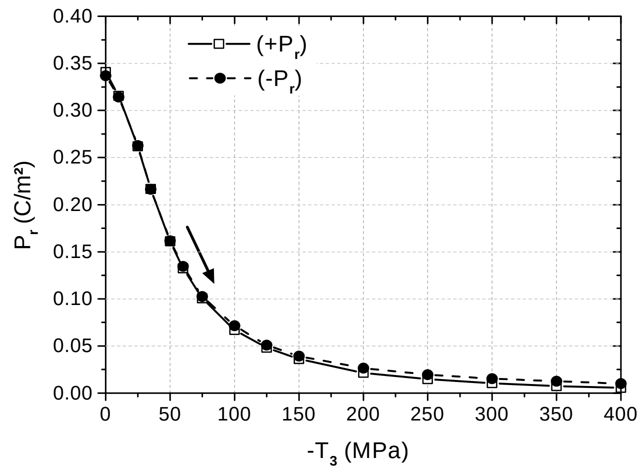


Fig. 4. Change in the positive and negative direction remnant polarization with increasing compressive stress preloads.

## 3. Results and discussion

### 3.1. *P–E curves as a function of preload stress*

The polarization versus electric field (*P–E*) hysteresis loops under different compressive stress preload levels are shown in Fig. 2.

We notice first that the area of these *P–E* hysteresis loops decreases with increasing preload stresses. The *P–E* hysteresis loop area represents the unit-volume polarization dissipation energy of a ferroelectric material subjected to one full cycle of electric field loading.[17] The change in polarization dissipation energy is plotted in Fig. 3 as a function of the preload stress, in which the dissipation energy is found to decrease non-linearly with the prestress increment.

The polarization dissipation energy is also termed energy loss being consumed for self-heating of the specimen and related directly to the amount of domains participating in the switching process during an electric field loading cycle. From Fig. 3 it is clear that the amount of domains contributing to polarization reversal decreases non-linearly with increasing prestress. In the stress-free state ($T = 0$ MPa), the dissipation energy is $1.382 \times 10^6$ J/m$^3$; at $-400$ MPa, the dissipation energy decreases to $0.043 \times 10^6$ J/m$^3$, which is approximately 30 times less than in the stress-free state. As is seen in Fig. 2, the corresponding *P–E* curve at $-400$ MPa nearly becomes a straight line with very low hysteresis, which implies that relatively few domains participate in polarization reversal under such high stress preload.

The *P–E* hysteresis loops in Fig. 2 show a pronounced decrease of remnant polarization, saturation polarization (at $\pm 2$ kV/mm), and coercive field as the compressive stress increases. The changes in the absolute values of remnant polarization and coercive field with increasing prestress are plotted in Figs. 4 and 5, respectively, where $+P_r$ and $-P_r$ symbolize remnant polarization in the positive and negative directions, respectively, and $+E_c$ and $-E_c$ are defined

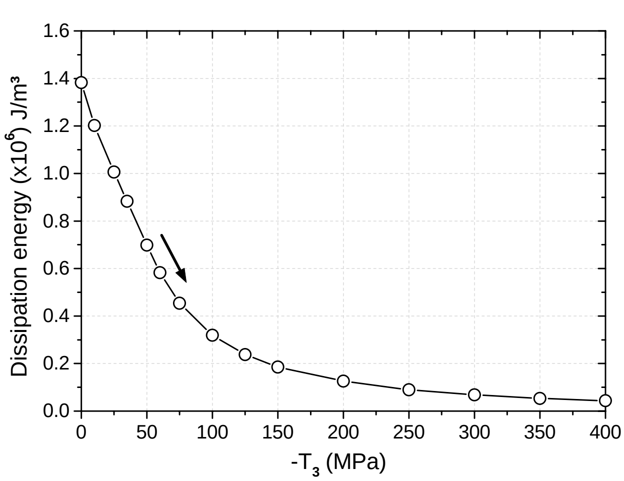


Fig. 3. Polarization dissipation energy (integration of the area of *P–E* hysteresis loops) as a function of compressive stress preload.

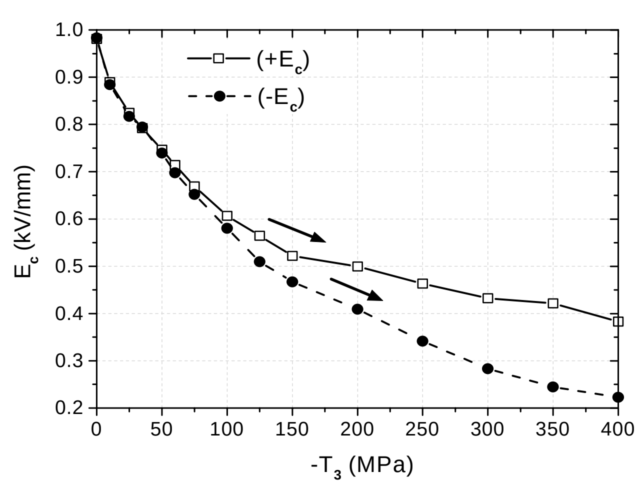


Fig. 5. Change in the positive and negative direction coercive fields with increasing compressive stress preloads.

as positive and negative direction coercive electric fields, respectively.

Apparently, both the remnant polarization and the coercive field decrease non-linearly with the increment in the superimposed compressive stress. For example, $+P_r$ is 0.341 C/m$^2$ in the stress-free state, and is now 0.006 C/m$^2$ at −400 MPa, while $-P_r$ is −0.337 C/m$^2$ at 0 MPa, decreasing to −0.010 C/m$^2$ at −400 MPa. In addition, approximately symmetrical changes in positive and negative remnant polarization can be observed in Fig. 4.

The positive direction coercive field ($+E_c$) is 0.981 kV/mm in the stress-free state, decreasing to 0.383 kV/mm at −400 MPa. $-E_c$ has the value of −0.983 kV/mm at 0 MPa, and is −0.223 kV/mm at −400 MPa. The plots of $\pm E_c$ in Fig. 5 indicate that the changes in the positive and negative direction coercive field with increasing preload stress appear not to be symmetrical. The negative direction coercive field ($-E_c$) decreases slightly more significantly than $+E_c$. This phenomenon was observed in repeated experiments.

The experimental results of the changes in remnant polarization and coercive field with increasing preload stress are in agreement with the observation by Lynch[20] for PLZT material.

The decrease of remnant polarization should be attributed to the depolarization induced by mechanical loading through non-180° ferroelastic domain switching processes, where domains are aligned orthogonally to the electric field applied. Summing up the plot of the dissipation energy in Fig. 3 we can conclude that, with compressive preload increasing, more and more domains are constrained by the prestress and cannot be reorientated by the electric field so as to participate in polarization reversal. Consequently, both remnant polarization and maximum polarization at ±2 kV/mm become continuously lower.

### 3.2. *S–E curves as a function of preload stress*

The longitudinal strain ($S_3$) and transverse strain ($S_1$) versus electric field "butterfly" curves were measured simultaneously at various prestress levels. The results are shown in Figs. 6 and 7, respectively.

One of the most notable features we can see from Figs. 6 and 7 is that, as the stress level is increased, the $S_3$–$E_3$ curves are shifted towards the negative strain direction and the $S_1$–$E_3$ curves are shifted towards the positive strain direction. We also find that the downward/upward dips in the longitudinal/transverse strain curves become rounded and eventually flatten out. There is very little electrically induced strain at much higher stress levels. In Fig. 8, non-linear changes in the residual longitudinal and transverse strains (strain values at $E = 0$ kV/mm) can be clearly observed with increasing stresses.

As was pointed out by Lynch,[20] the superimposed compressive stress makes two contributions to the total strain response. First, it induces elastic deformation, which will shift the longitudinal strain curves downward and move the transverse strain curves upward. The second contribution made by the preload stress is ferroelastic non-180° domain switching. Besides the effect of shifting the strain curves, stress-induced ferroelastic domain switching also has a significant impact on the shapes of the polarization and strain hysteresis loops, dielectric permittivity, and piezoelectric coefficients.

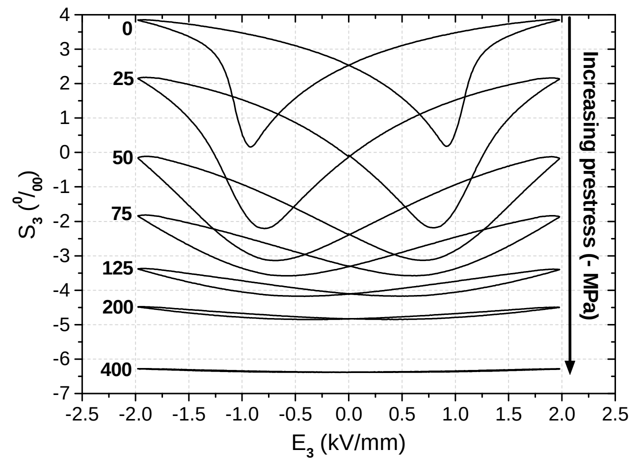


Fig. 6. Longitudinal strain vs. electric field ($S_3$–$E_3$) curves as a function of compressive stress preload.

### 3.3. *$\varepsilon_{33}$, $d_{33}$, and $d_{31}$ as a function of preload stress*

At different prestress levels, the dielectric permittivity was calculated approximately by using Eq. (1), which gives

$$\varepsilon_{33}(T) = \frac{\Delta D_3}{\Delta E_3} \quad (1)$$

where $\Delta D_3$ is the polarization difference between −0.1 and +0.1 kV/mm. Within such a small field range, the calculated $\varepsilon_{33}$ is nearly equivalent to the slope of the $P$–$E$ curve as the electric field passes through zero. The calculated dielectric constant can be called differential permittivity, which

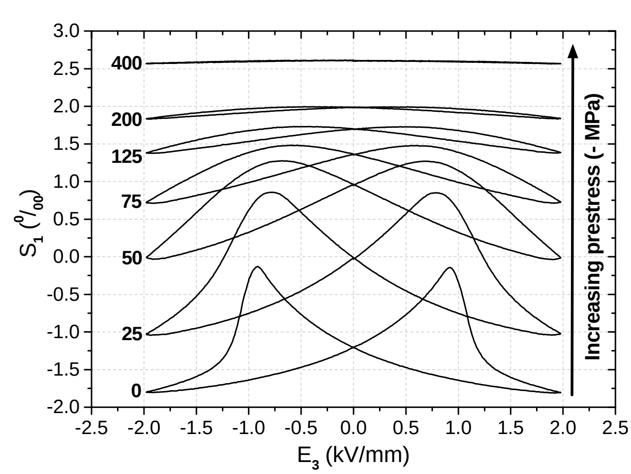


Fig. 7. Transverse strain vs. electric field ($S_1$–$E_3$) curves as a function of compressive stress preload.

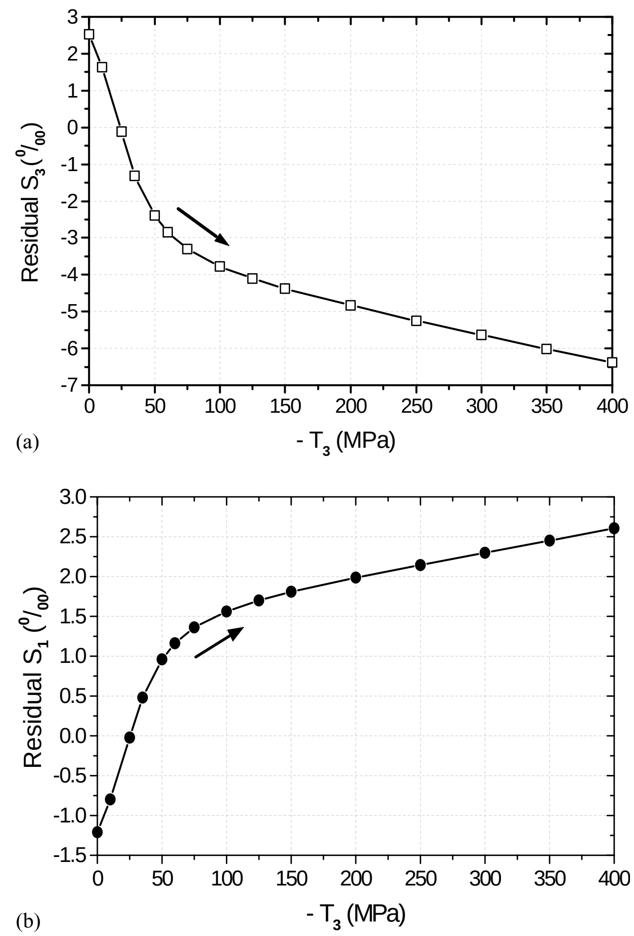


Fig. 8. Longitudinal (a) and transverse (b) residual strains (strain values at $E = 0$ kV/mm) as a function of compressive stress preload.

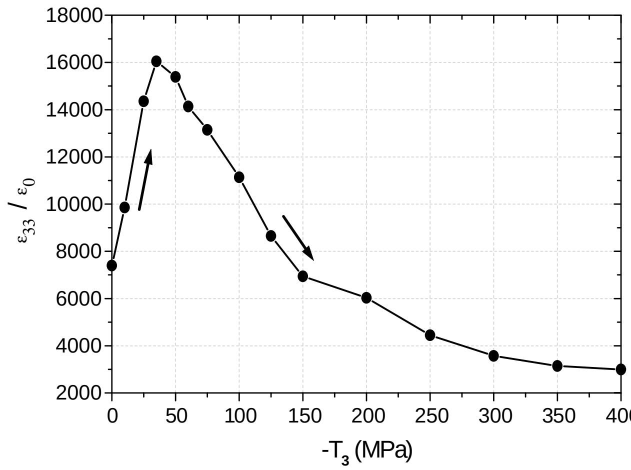


Fig. 9. Change in the relative dielectric constant (measured from the slope of *P*–*E* curves as the *E* field passes through 0 kV/mm) with increasing preload stresses.

includes both the reversible (intrinsic dielectric property) and irreversible (extrinsic domain switching related property) contributions of the material. Generally, the differential dielectric constant is significantly higher than the permittivity measured by a dynamic method, which is normally achieved by measuring the response of a material to a low ac signal superimposed on a substantial dc bias signal. The dynamic coefficients are mainly determined by the reversible effects.[25]

The change in the differential dielectric constant is illustrated in Fig. 9 as a function of the preload stress.

We can see that the magnitude of the differential $\varepsilon_{33}$ depends significantly on the preload stress levels. The relative dielectric constant is approximately 7400 in the stress-free state. Initially, it increases with increasing stress; after reaching a maximum value of $\varepsilon_{33}/\varepsilon_0 \approx 16{,}000$ at $-35$ MPa, it gradually decreases with further prestress increments. At $-400$ MPa, nearly all domains have been aligned orthogonally to the field applied, and the corresponding relative permittivity is around 3000. The experimental results indicate that the preload stress has a significant influence on the dielectric property of a ferroelectric material.

Similar to $\varepsilon_{33}$, two important piezoelectric constants, $d_{33}$ and $d_{31}$, were calculated at different prestress levels by Eq. (2), which gives

$$d_{33}(T) = \frac{\Delta S_3}{\Delta E_3}$$
$$d_{31}(T) = \frac{\Delta S_1}{\Delta E_3} \qquad (2)$$

Again, the electric field range was limited between $-0.1$ and $+0.1$ kV/mm. Within such a narrow range, the calculated $d_{33}$ and $d_{31}$ are nearly equal to the slopes of the $S_3$–$E_3$ and $S_1$–$E_3$ curves as the electric field passes through zero.

The changes in $d_{33}$ and $d_{31}$ are plotted in Fig. 10 as a function of prestress. In the stress-free state, the calculations furnish $d_{33} = 1470$ and $d_{31} = -670$. Both $d_{33}$ and $d_{31}$ initially increase with the preload stress increasing, reaching their peak levels of $d_{33} = 2380$ and $d_{31} = -1050$ at $-25$ MPa. Thereafter, $d_{33}$ and $d_{31}$ decrease quickly with further preload increase and finally approach zero, which indicates that there is hardly any piezoelectric effect under such high compressive stress preload, in this experiment, e.g., from $-300$ to $-400$ MPa.

### 3.4. Discussion

The influence of the preload stress on the shapes of the *P*–*E* and *S*–*E* curves can be explained by two successive non-180° domain switching processes. Chaplya and Carman[21] presented a similar explanation in one of their recent publications. In the stress-free state, when the *E* field drops from +2 to 0 kV/mm, most of the domains are preserved with their orientations parallel to the positive electric field loading direction (only a few unstable domains switch back to their initially unpolarized states). From 0 kV/mm, the first non-180° domain switching process starts in the material as a negative electric field is applied. When the negative coercive field ($-E_c$) is reached, the first non-180°

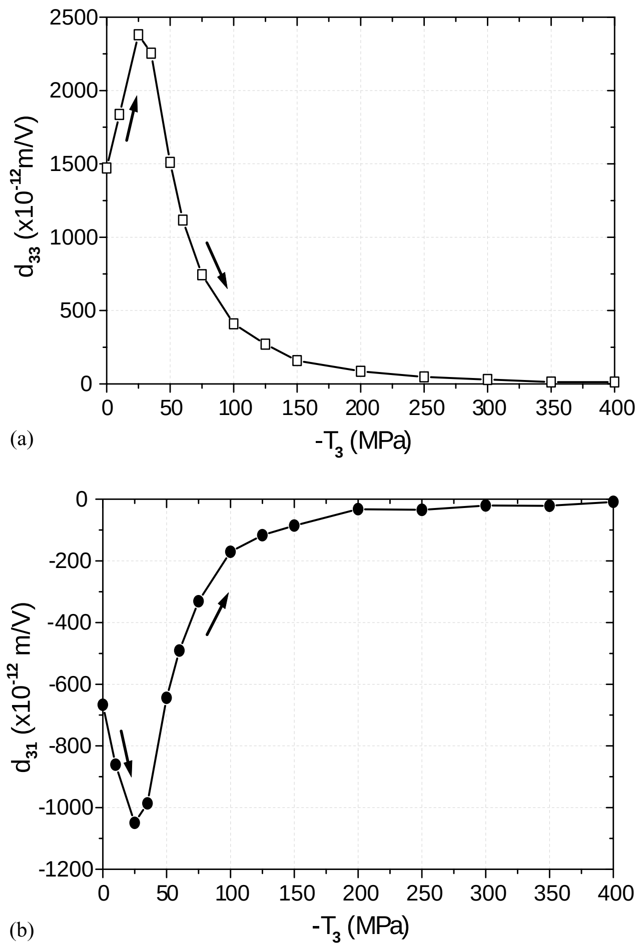


Fig. 10. Change in the piezoelectric coefficients $d_{33}$ (a) and $d_{31}$ (b) with increasing preload stresses. The piezoelectric constants were measured from the slopes of the $S_3$–$E_3$ and $S_1$–$E_3$ curves as the electric field passed through 0 kV/mm.

switching process will be completed. The strain is found to achieve its minimum absolute value, and polarization is zero. After $-E_c$, the second non-180° domain switching process begins, both polarization and strain are observed to increase by "jumps," and finally become saturated at higher electric field levels. (To simplify the discussion, it is assumed here that polarization and strain reach their minimum levels simultaneously. For a detailed discussion of this aspect, see Refs. 19,23.)

When a low compressive stress is superimposed on the specimen (e.g., −25 or −50 MPa), the shapes of the *P*–*E* and *S*–*E* curves are different from those in the stress-free state. Due to compression load-induced depolarization, the resultant polarization and strain at maximum *E* field (±2 kV/mm) seem to become lower. As discussed earlier, this is because some of the domains have been constrained orthogonally to the *E* field by the superimposed stress and cannot be reorientated by the electric field with the maximum amplitude of ±2 kV/mm in this experiment. During the field unloading period from +2 to 0 kV/mm, the preload stress will induce part of the first non-180° domain switching even before 0 kV/mm. As a result, we can see both polarization and strain decrease more drastically than in the stress-free state. After 0 kV/mm, the negative *E* field acts together with the prestress to complete the residual first non-180° switching. Until the negative coercive field ($-E_c$) is reached, polarization and strain reach their minimum values.

The magnitude of the coercive field with a compressive stress preload is smaller than it is in the stress-free state. This is due to three reasons: (1) fewer domains take part in polarization reversal, (2) the preload stress destabilizes the polarized state and leads to part of the first non-180° domain switching in the period of electric field unloading from ±2 to 0 kV/mm, (3) the first non-180° switching process is completed by the combined action of the *E* field and prestress.

After $-E_c$, the steadily increasing electric field load will act against the prestress to induce the second non-180° domain switching. Consequently, polarization and strain experience a more gradual development rather than a "jump" in the case of $T = 0$ MPa. With further preload stress increments, fewer and fewer domains take part in polarization reversal, and the resultant *P*–*E* and *S*–*E* curves become flat. For example, at −400 MPa, the *P*–*E* curve approximates a straight line, and hardly any electrically induced strain change can be observed.

So far, the influences of compressive prestress on the polarization and strain versus electric field curves have been clarified. From the plots of $\varepsilon_{33}$, $d_{33}$, and $d_{31}$ as a function of the preload stress we can see that the superimposed stress also has a significant impact on the piezoelectric and dielectric properties of a piezoceramic material. The general observation is that the coefficients investigated initially increase with increasing preload stress; after reaching a maximum value at a specific low stress level they decrease quickly with further stress increases.

In our other experimental investigation,[26] unipolar high electric field-induced polarization and strain were measured for this soft PZT material under various compressive stress preloads of up to −400 MPa. The results also indicated a significant enhancement of dielectric and piezoelectric properties within a certain prestress loading range. The enhanced performance may be attributable to the extra contribution by the extrinsic material properties to the overall dielectric/piezoelectric response, i.e., more non-180° domain switching induced by combined electromechanical loading. Recently, a similar phenomenon was reported by several authors in their measurements of soft/hard piezoceramics or piezoelectric stack actuators.[8,9,25] The enhanced actuation performance must be addressed in the design and practical application of active actuators.

## 4. Summary and conclusions

In this study, a special method of specimen preparation and an improved experimental setup were developed to investigate reliably the large-signal electromechanical response of piezoceramics. Bipolar high electric field-induced polarization and "butterfly" longitudinal/transverse strain hysteresis loops were directly measured for a commercial soft PZT material under various compressive stress preloads of up to −400 MPa. As the compressive stress prevented full alignment of the domains and induced mechanical depolarization, hysteresis of the *P–E* curves became less and less pronounced and both remnant polarization and coercive field decreased non-linearly with the superimposed stress increasing. Mechanical preload induced elastic deformation and ferroelastic domain switching significantly changed the shape and amplitude of the strain curves. With the prestress increment, the strain curves became much smoother, and non-linear changes in the residual strain (strain values at zero electric field) were observed. At much higher stress levels, the *P–E* curves became a nearly straight line, and hardly any electrically induced strain variation was observed. Slopes of the polarization and strain curves at zero electric field were measured to evaluate the influence of prestress on the permittivity ($\varepsilon_{33}$) and piezoelectric coefficients ($d_{33}$ and $d_{31}$) of piezoceramics. Significant enhancement of the dielectric and piezoelectric performance was observed within a narrow prestress range. After reaching their maximum values at a certain stress level, these parameters decreased rapidly as compression preload increased further. The material displayed hardly any piezoeffects at much higher stress levels (e.g., ≥300 MPa). The experimental results were interpreted qualitatively in terms of two successive non-180° domain switching processes induced by combined electromechanical loading.

## Acknowledgements

The financial support of this work by the German Research Foundation (DFG) is gratefully acknowledged.

## References

1. Akhras, G., Smart materials and smart systems for the future. *Can. Mil. J.* 2000, Autumn, 25–32.
2. Uchino, K., *Ferroelectric Devices*. New York, Marcel Dekker, 2000.
3. Haertling, G. H., Ferroelectric ceramics: history and technology. *J. Am. Ceram. Soc.* 1999, **82**(4), 797–818.
4. Jaffe, B., Cook, W. R. and Jaffe, H., *Piezoelectric Ceramics*. Academic Press, New York, 1971.
5. Xu, Y., *Ferroelectric Materials and Their Applications*. North Holland, 1991.
6. Zhang, Q. M., Pan, W. Y., Jang, S. J. and Cross, L. E., Domain wall excitations and their contributions to the weak-signal response of doped lead zirconate titanate ceramics. *J. Appl. Phys.* 1988, **64**, 6445–6451.
7. IEEE Standard on Piezoelectricity, *ANSI/IEEE Std. 176-1987*. IEEE, New York, NY, 1988.
8. Viehland, D., Tito, F., McLaughlin, E., Robinson, H., Janus, R., Ewart, L. *et al.*, Enhancement of electromechanical coupling coefficient and acoustic power density in conventional "hard" $Pb(Zr_{1-x}Ti_x)O_3$ ceramics by application of uniaxial stress. *J. Appl. Phys.* 2001, **90**(3), 1496–1500.
9. Mitrovic, M., Carman, G. P. and Straub, F. K., Response of piezoelectric stack actuators under combined electro-mechanical loading. *Int. J. Solids Struct.* 2001, **38**, 4357–4374.
10. Straub, F. K. and Merkley, D. J., Design of a smart material actuator for rotor control. In *Proceedings of SPIE: Smart Structures and Integrated Systems 1995, Vol 2443*. San Diego, CA, 1995, pp. 89–104.
11. Cao, H. and Evans, A. G., Nonlinear deformation of ferroelectric ceramics. *J. Am. Ceram. Soc.* 1993, **76**(4), 890–896.
12. Schäufele, A.B. and Härdtl, K.H., Ferroelastic properties of lead zirconate titanate ceramics. *J. Am. Ceram. Soc.* 1996, **79**(10), 2637–2640.
13. Huber, J. E., Shieh, J. and Fleck, N. A., Multiaxial response of hard and soft ferroelectrics under stress and electric field. In *Proceedings of SPIE: Smart Structures and Materials 2002, Vol 4699*, ed. C. S. Lynch. San Diego, CA, 2002, pp. 133–142.
14. Kamlah, M., Ferroelectric and ferroelastic piezoceramics-modeling of electromechanical hysteresis phenomena. *Continuum Mech. Thermodyn.* 2001, **13**(4), 219–268.
15. Fett, T., Müller, S., Munz, D. and Thun, G., Nonsymmetry in the deformation behaviour of PZT. *J. Mater. Sci. Lett.* 1998, **17**, 261–265.
16. Fett, T., Munz, D. and Thun, G., Young's modulus of soft PZT from partial unloading tests. *Ferroelectrics* 2002, **274**, 67–81.
17. Lines, M. E. and Glass, A. M., *Principles and Applications of Ferroelectrics and Related Materials*. Oxford, 1977.
18. Viehland, D. and Chen, Y.-H., Random-field model for ferroelectric domain dynamics and polarization reversal. *J. Appl. Phys.* 2000, **88**, 6696–6707.
19. Zhou, D. Y., Kamlah, M. and Munz, D., Rate dependence of soft PZT ceramics under electric field loading. In *Proceedings of SPIE: Smart Structures and Materials 2001, Vol 4333*, ed. C. S. Lynch. New Port Beach, CA, 2001, pp. 64–70.
20. Lynch, C. S., The effect of uniaxial stress on the electro-mechanical response of 8/65/35 PLZT. *Acta Mater.* 1996, **44**(10), 4137–4148.
21. Chaplya, P. M. and Carman, G. P., Dielectric and piezoelectric response of lead zirconate-lead titanate at high electric and mechanical loads in terms of non-180° domain wall motion. *J. Appl. Phys.* 2001, **90**(10), 5278–5286.
22. Nuffer, J., Lupascu, D. C. and Rödel, J., Damage evolution in ferroelectric PZT induced by bipolar electric cycling. *Acta Mater.* 2000, **48**, 3783–3794.
23. Zhou, D. Y., *Experimental Investigation of Non-Linear Constitutive Behavior of PZT Piezoceramics*. Ph.D. thesis, University Karlsruhe, 2003.
24. Munz, D. and Fett, T., *Ceramics-Mechanical Properties, Failure Behaviour, Materials Selection.* Springer Series in Materials Science, Springer-Verlag, Berlin, 1999.
25. Yang, G., Liu, S.-F., Ren, W. and Mukherjee, B. K., Uniaxial stress dependence of the piezoelectric properties of lead zirconate titanate ceramics. In *Proceedings of SPIE: Smart Structures and Materials 2000, Vol 3992*, ed. C. S. Lynch. New Port Beach, CA, 2000, pp. 103–113.
26. Zhou, D. Y., Kamlah, M. and Munz, D., Uniaxial compressive stress dependence of the high-field dielectric and piezoelectric performance of soft PZT piezoceramics. *J. Mater. Res.* 2004, **19**(3), 834–842.